

Theoretical Model of a New Type Tunneling Transistor

P. PFEFFER*

Institute of Physics, Polish Academy of Sciences, al. Lotnikow 32/46, PL-02668 Warsaw, Poland

Received: 04.05.2023 & Accepted: 10.07.2023

Doi: [10.12693/APhysPolA.144.137](https://doi.org/10.12693/APhysPolA.144.137)

*e-mail: pfeffer@ifpan.edu.pl

A tunneling transistor without heterojunction as a theoretical design, or more precisely, the controlled transmission of an electron current through barrier potential, is under consideration. Electrons from the conduction band of the source tunnel through the forbidden gap E_g of the channel to the conduction band of the drain. Calculations of the tunneling current J made at helium temperature for the example structures InAs–InAs–InAs, Au–GaSe–Au, and Al–AlN–Al show that for a constant source–drain voltage, V_C , of several mV, changes in the gate voltage, V_G , applied to the channel within the voltage range of $0-E_g/2e$, change J by even 10 orders of magnitude. Unlike existing solutions, such as the tunnel field-effect transistor, the proposed device uses the change of V_G (gate voltage), i.e., a change in the electrostatic potential in the channel, to modify the imaginary wave vector k_z of tunnel current electrons. Consequently, the gate voltage controls the damping force of the electron wave functions and thus the magnitude of the tunneling current, J . The effect of increasing temperature T on the relation $J(V_G)$ is also tested. It is found that only in the structures with a wide forbidden channel gap this effect is insignificant (at least up to $T = 300$ K).

topics: transistor, tunneling, bandgap, wave vector

1. Introduction

The tunnel current in the metal–insulator–metal (M-I-M) structure has been theoretically described and experimentally tested for many years, starting from 1930 [1] (see also, e.g., [2–7]). The theoretical problem of transmission of relativistic electrons through the potential barrier of a controlled height, described by the Dirac equation, called the Klein paradox, was published [8] and resolved many years ago, see review [9]. A similar theoretical problem, in close analogy to the Dirac model, but for transmission coefficient of conduction electrons through the potential barrier with the height depending on the voltage applied to it, V_G (gate potential), was solved for graphene [10], for phosphorus [11], and for IV–VI semiconductor compounds [12] in recent years. The same mechanism for controlling the current density depending on the amount of V_G is used in the existing field-effect transistors (TFETs). Both of these phenomena are the basis of the proposed theoretical tunneling transistor model, the general scheme of which is shown in Fig. 1. Nevertheless, the design under consideration, described below, differs from the TFET solutions based on the fact that an increase in V_G means an increase in the bands bending in the source–channel heterojunction and, as a result, an increase in the tunnel current J from the valence band to the conduction band in the $p^+ - i - n^+$

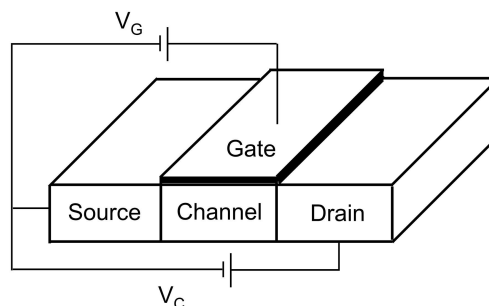


Fig. 1. Scheme of the proposed transistor model; V_C is the voltage applied between Source and Drain and V_G is the Gate voltage applied through the oxide layer to the Channel.

or $p^{++} - n^- - n^+$ configuration or from the conduction band to the valence band in the $n^+ - i - p^+$ or $n^{++} - p^- - p^+$ configuration (band-to-band tunneling (BTBT)), see, e.g., [13–18].

2. Tunneling current in metal–insulator–metal structure

Here we consider the details of the general formula for the dependence of the current J on the applied voltage V_C in the M-I-M structure (see [3]) as

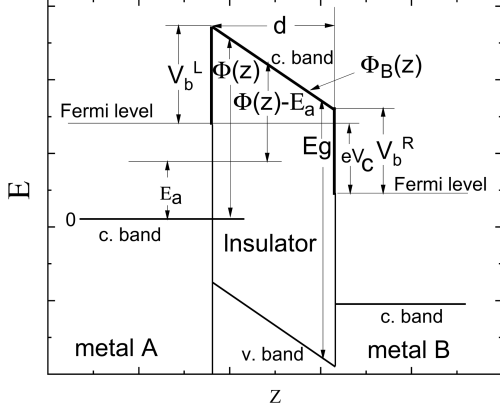


Fig. 2. Diagram of the metal–insulator–metal structure with applied voltage V_C between metal A and metal B (see, e.g., [3]). The tunneling current flows along the z -direction from metal A through the forbidden gap of the insulator to metal B; V_b^L and V_b^R are the band offsets between the conduction band of the insulator and the Fermi energy E_F in metal A or metal B, respectively; E_a is the energy of the electron.

the Source–Channel–Drain structure in our design. The elements of this structure are selected so that current electrons from the metal A tunnel along the z -direction through the forbidden gap of the insulator to the metal B, see Fig. 2. The trapezoidal potential of the insulator used in the theoretical description is an effective approximation of the potential, as is the two-band model for calculating the energy $E(k)$ of an electron, see, e.g., [4–7]. The wave vector $k_z(z)$ of the tunneling electrons has a decisive influence on the magnitude of the current J . This vector has an imaginary value and determines how much the electron wave function is damped in the insulator area.

In order to determine the formula for $|k_z(z)|$, we proceed as follows. The energy of the electron in the insulator, $E(k)$, counted from the bottom of the forbidden gap, in the two-band model, is

$$E(k) = E_g - (\Phi(z) - E_a) = \frac{E_g}{2} \pm \sqrt{\left(\frac{E_g}{2}\right)^2 + \frac{E_g \hbar^2 [(k_z^i)^2 + k_\perp^2]}{2m_0^*}}, \quad (1)$$

where E_g is the forbidden gap of the insulator; $k^2 = k_\perp^2 + (k_z^i)^2$, and the wave vector k_\perp is real, and the wave vector k_z^i is purely imaginary ($k_z^i = k_z = i|k_z|$); E_a is the energy of the electron in metal A; m_0^* is the effective electron mass of m_C at the conduction-band edge or m_V at the valence-band edge, corresponding to the sign in front of the square root in (1); and V_C is the applied voltage. As in Fig. 2, $\Phi(z) = \Phi_B(z) + E_F$ is the energy of the M-I-M barrier potential relating to the metal A conduction band edge, where

$$\Phi_B(z) = V_b^L + (V_b^R - V_b^L - eV_C) \frac{z}{d}. \quad (2)$$

Here, V_b^L and V_b^R are metal–insulator barrier energies, and E_F is the Fermi energy.

Hence,

$$|k_z(z)| = \left[\left(1 - \frac{\Phi(z) - E_a}{E_g}\right) (\Phi(z) - E_a) \frac{2m_0^*}{\hbar^2} + k_\perp^2 \right]^{\frac{1}{2}}, \quad (3)$$

or

$$|k_z(z)| = \left[\left(1 - \frac{E(z)}{E_g}\right) E(z) \frac{2m_0^*}{\hbar^2} + k_\perp^2 \right]^{\frac{1}{2}}. \quad (4)$$

The next step is the general expression for the elastic tunneling current $J(V_C)$ from metal A to metal B (see, e.g., [5]),

$$J(V_C) = \frac{2eS}{\hbar} \int_0^\infty dE_a (f_A(E_a) - f_B(E_a)) \int_0^\infty \frac{d^2 k_\perp}{(2\pi)^2} \exp \left[-2 \int_0^d dz |k_z(z)| \right] = \frac{eS}{\pi \hbar} \int_0^\infty dE_a (f_A(E_a) - f_B(E_a)) \int_0^\infty dk_\perp k_\perp \exp \left[-2 \int_0^d dz |k_z(z)| \right], \quad (5)$$

or

$$\frac{J(V_C)}{S} \left[\frac{\text{A}}{\text{cm}^2} \right] = \frac{7.7483}{10^5} \int_0^\infty dE_a (f_A(E_a) - f_B(E_a)) \times \int_0^{k_\perp^M} dk_\perp k_\perp \exp \left[-2 \int_0^d dz |k_z(z)| \right], \quad (6)$$

where $k_\perp^M = k_\perp^F$ for E_F and $k_z=0$ in the M-I-M system. Further, d is the insulator thickness, and S is the area of the interface between the metal and the insulator. The terms $f_A(E_a)$ and $f_B(E_a)$ are the Fermi–Dirac (F-D) distribution functions for metal A and metal B, respectively, $f_A(E_a) = 1/[1 + \exp((E_a - E_a^F)/(k_B T))]$ and $f_B(E_a) = 1/[1 + \exp[(E_a - (E_a^F - eV_C))/(k_B T)]]$.

For very low temperatures, one has

$$J(V_C) \left[\frac{\text{A}}{\text{cm}^2} \right] = \frac{7.7483}{10^5} \int_{E_F - eV}^{E_F} dE_a \int_0^{k_\perp^M} dk_\perp k_\perp \exp \left[-2 \int_0^d dz |k_z(z)| \right]. \quad (7)$$

One can notice that the formula for $J(V_C)$ is dominated by the element with the exponential decay, which is a result of the imaginary value of k_z in the electron wave function for the insulator forbidden gap. It is also seen that all electrons in metal A with energy in the range $E_F - (E_F - eV_C)$ form a tunneling current from metal A to metal B. Furthermore, the tunneling current of the electron is the greater, the smaller $|k_z|$ it has.

3. Dependence of current electrons energy on k_z^2 in the forbidden gap of the channel

Henceforth, the term metal–insulator–metal is replaced by the term Source–Channel–Drain; Source and Drain are metals or n -type semiconductors, and Channel is a wide, medium, or narrow gap semiconductor (see Fig. 1).

Comparison of experimental data with theoretical calculations of $J(V_C)$ in the structure under consideration shows that to describe the dispersion $E(k_z^2)$ of electronic states in the forbidden gap of a channel, for example, InAs, GaSe, or AlN, the two-band model is good enough, see [4–6]. The knowledge of the dependence of E on k_z^2 for $k_\perp = 0$ is most important, because the greater k_\perp , the greater $|k_z|$ to keep the electron energy unchanged. On the other hand, the tunnel current is determined by electrons with $|k_z|$ as small as possible, i.e., with the damping of their wave function as little as possible.

If the effective masses of electrons m_C and holes m_V are not equal, the use of the two-band Franz model for band-to-band tunneling (see [19] and [20]) allows for a more detailed description of the tunneling process. It means replacing m_0^* in (1) by m_{Fr} , the value of which depends on the electron energy E in the band forbidden gap. The form of m_{Fr} is the following

$$m_{Fr}(E) = \frac{m_C}{\frac{E}{E_g} \left(1 - \frac{m_C}{m_V} \right) + \frac{m_C}{m_V}}, \quad (8)$$

where $E = E_g - \Phi(z) + E_a$, see Fig. 2. It is seen that for $E = 0$, one has $m_{Fr} = m_V$, and for $E = E_g - m_{Fr} = m_C$.

To calculate the energy dispersion $E(k_z^2)$ in the forbidden gap of GaSe for $k_\perp = 0$, we used (3) with $m_0^* = m_{Fr}$ and the GaSe parameters: $E_g = 2$ eV, $m_C/m_0 = 0.35$, and $m_V/m_0 = 0.07$ [5]. The curves calculated for $m_0^* = m_{Fr}$, $m_0^* = m_C$, and $m_0^* = m_V$ are shown in Fig. 4. From the comparison of the curves, it follows that the use of $m_{Fr}(E)$

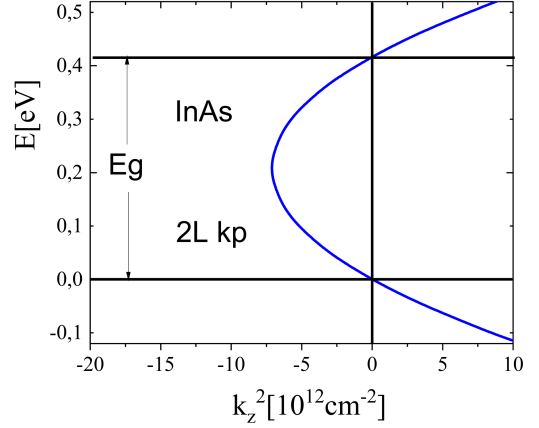


Fig. 3. Theoretical energy dispersion $E(k_z^2)$ in the forbidden gap of InAs for $k_\perp = 0$ calculated in the two-level model for $E_g = 0.417$ eV and $m_0^*/m_0 = 0.026$.

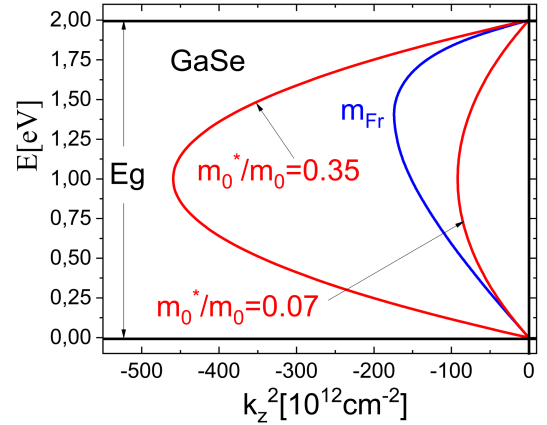


Fig. 4. Theoretical energy dispersions $E(k_z^2)$ in the forbidden gap of GaSe for $k_\perp = 0$. The blue curve includes the electron mass $m_{Fr}(E)$ calculated in the two-level Franz model for $m_C/m_0 = 0.35$, $m_V/m_0 = 0.07$ and $E_g = 2$ eV. The red curves are calculated in the two-level model for $m_C/m_0 = m_V/m_0 = m_0^*/m_0 = 0.35$ or 0.07 .

is necessary. The results of similar calculations for InAs and AlN are shown in Figs. 3 and 5, respectively. The InAs parameters are $E_g = 0.417$ eV and $m_0^*/m_0 = 0.026$ [21], while the AlN parameters are $E_g = 4.2$ eV and $m_0^*/m_0 = 0.45$ [6]. Figures 3–5 show that a slight change in the energy of the electron in the band gap significantly changes the value k_z^2 of the electron, i.e., changes its importance in the formation of the tunnel current.

4. Principles of operation of the proposed tunneling transistor

The basis of the proposed transistor is the observation that the current that flows through the Source–Channel–Drain structure biased with the constant voltage V_C can be changed depending on

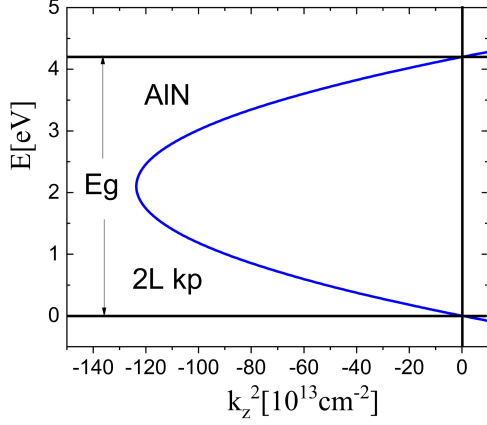


Fig. 5. Theoretical energy dispersion $E(k_z^2)$ in the forbidden gap of AlN for $k_\perp = 0$ calculated in the two-level model for $E_g = 4.2$ eV and $m_0^*/m_0 = 0.45$.

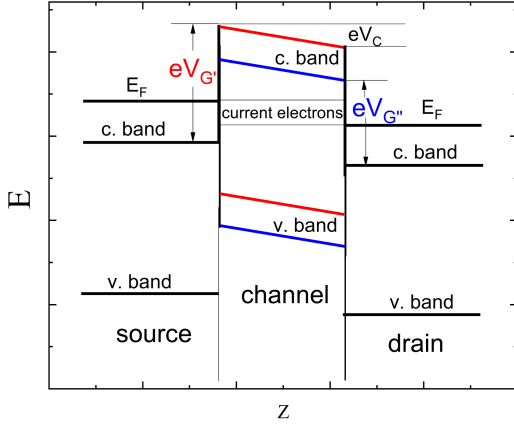


Fig. 6. Scheme of the proposed tunneling transistor for the Source–Drain voltage V_C and for two different values of the gate voltage $V_{G'}$ and $V_{G''}$ applied to the Channel. It is seen that the current electrons with energy in the range $E_F - (E_F - eV_C)$ tunnel through a barrier with a V_G -dependent height, i.e., through energetically different parts of the forbidden gap of the Channel.

the magnitude of the gate voltage V_G applied to the channel by an electrode separated from the channel by an oxide layer, see, e.g., [10]. In other words, by increasing or lowering the potential energy of the channel in relation to the source, we can control k_z^2 of the current electrons and thus the magnitude of the tunneling current, see Figs. 3–5 and 6. So, the modified formula for $|k_z(z)|^2$ of an electron in the forbidden channel gap with the applied voltage V_G looks like this

$$|k_z(z)|^2 = \left(1 - \frac{E(z) - eV_G}{E_g}\right) (E(z) - eV_G) \frac{2m_0^*}{\hbar^2} + k_\perp^2. \quad (9)$$

The dependences $J(V_G)$ for structures InAs–InAs–InAs, Au–GaSe–Au, and Al–AlN–Al calculated using (7) and (9), i.e., at helium temperature,

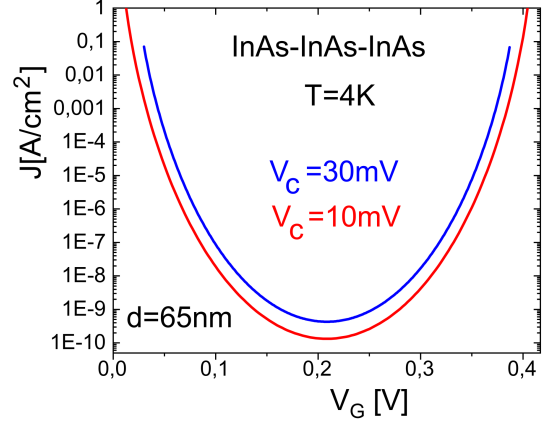


Fig. 7. Theoretical tunneling current J versus gate voltage V_G applied to the InAs barrier. The curves are calculated for values of voltage $V_C = 30$ mV and 10 mV applied to the InAs–InAs–InAs structure with the barrier width $d = 65$ nm. For V_G in the range $V_C - (E_g/e - V_C)$, the electrons tunnel through the whole width of the InAs forbidden gap, see Fig. 2. A change of the value of V_G shifts the InAs barrier on the energy axis, thereby changing the value of energy, $E(k_z)$, and the value of the wave vector, k_z , of tunneling electrons in the forbidden gap (see Fig. 3), and, as a result, leads to the exponential change in the value of the tunneling current (see (6)). It is seen that a slight change of V_G can change the value of the tunneling current J by a few orders of magnitude.

are presented in Figs. 7–9. A negative or positive value of V_G applied to the GaSe element in the Au–GaSe–Au structure or to the AlN element in the Al–AlN–Al structure means a reduction or increase in the virtual shift of V_b^L and V_b^R of the GaSe barrier with respect to the Au source or the AlN barrier with respect to the Al source, thereby changing k_z^2 of current electrons. The obvious relationship that the wider the channel, the smaller the minimum tunnel current J , is shown in Fig. 9. Comparing the relationship $J(V_G)$ with $E(k_z^2)$ (Figs. 3–5) for these structures, we see that the wider the channel bandgap is, the greater range of k_z values it has, and thus a greater range of tunnel current changes is possible.

The conclusion that can be drawn from the $J(V_G)$ curves in Figs. 7–9 is as follows: the smaller V_C , the greater the ratio of the maximum tunnel current J_{\max} to the minimum tunnel current J_{\min} . The reason is that the smaller V_C and, consequently, J_C are, the fewer electrons form the current, and the smaller the difference between $|k_z|^2$ of these electrons is. Thus, the highest ratio of J_{\max} to J_{\min} for a given width d will occur when the voltage V_C is extremely small, i.e., when the tunneling current is formed exclusively from electrons of the same energy E . In this case, it is convenient to calculate the transmission coefficient TC of electrons tunneling

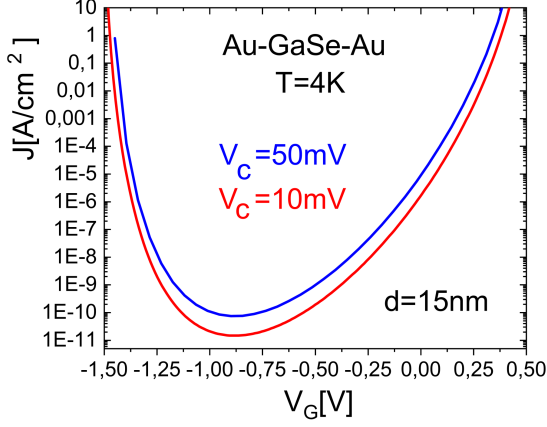


Fig. 8. Theoretical tunneling current J versus gate voltage V_G applied to the GaSe barrier. The curves are calculated for the voltage values $V_C = 50$ and 10 meV applied to the Au–GaSe–Au structure. The width of the GaSe barrier $d = 15$ nm and $V_b^L = V_b^R = 1.48$ eV are used. The asymmetrical shape of the curves is the result of the asymmetry energy dispersion $E(k_z^2)$ in the forbidden gap of GaSe (see Fig. 4).

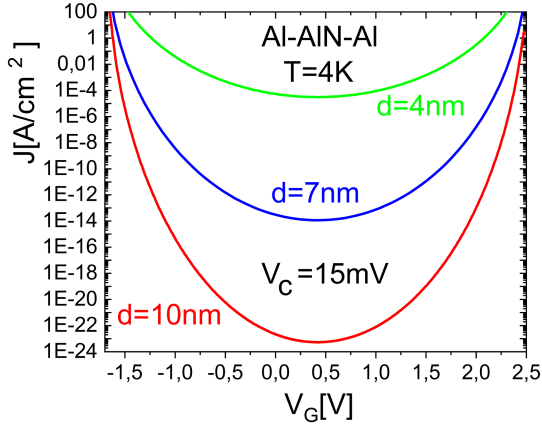


Fig. 9. Theoretical tunneling current J versus gate voltage V_G applied to the AlN barrier. The curves are calculated for the voltage value $V_C = 15$ mV applied to the Al–AlN–Al structure. The widths of the barrier $d = 4, 7,$ and 10 nm and $V_b^L = V_b^R = 1.68$ eV are used.

through the forbidden gap of the channel vs V_G (the procedure is included, e.g., in [12]). Such a dependence $TC(V_G)$ for the InAs–InAs–InAs structure is shown in Fig. 10. It can be seen that the ratio of TC_{\max} to TC_{\min} , and therefore J_{\max} to J_{\min} , is indeed extremely large.

5. Dependence of the $J(V_G)$ characteristic on temperature

With increasing temperature, according to the Fermi–Dirac distribution function f_{F-D} , the number of electrons with energy greater than E_F

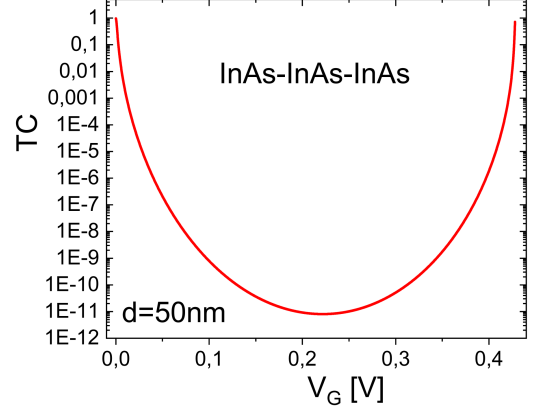


Fig. 10. Transmission probability TC for electrons with a specific value of E within forbidden gap of InAs versus barrier voltage V_G . The curve is calculated for values of V_G in the range $0 - E_g/e$.

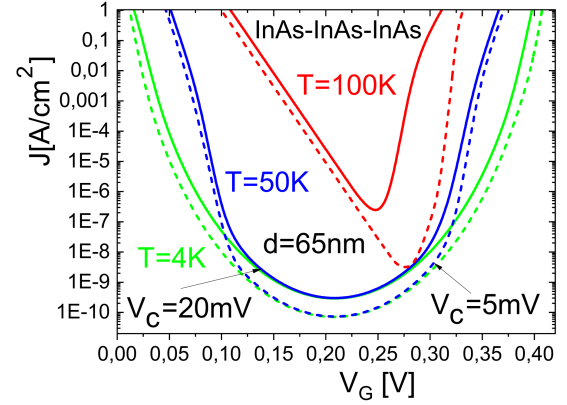


Fig. 11. Theoretical tunneling current J versus gate voltage V_G , calculated for different values of temperature for the structure InAs–InAs–InAs, i.e., with narrow gap channel, for applied voltage $V_C = 20$ mV (solid lines), and for $V_C = 5$ mV (dashed lines). The InAs channel forbidden gap $E_g = 0.417$ eV and its width $d = 15$ nm are used. It is seen that the change in $J(V_G)$ characteristic with increasing temperature above $T = 50$ K becomes more and more significant.

increases. This means that the increasing number of electrons passes through the channel of the investigated structure not through the bandgap, but through its conduction band. This, in turn, means that the contribution of tunneling electrons to the total current, J , decreases the more, the narrower the forbidden gap of the channel is. As a result, the $J(V_G)$ characteristic calculated using (6) in the example structure with a narrow band gap channel changes significantly for the temperature above $T = 50$ K, see Fig. 11. In the structure with a medium band gap, $J(V_G)$ changes significantly for the temperature above about $T = 200$ K, see Fig. 12. While in the structure with a wide band gap studied up to $T = 300$ K, $J(V_G)$ changes slightly, see Fig. 13.

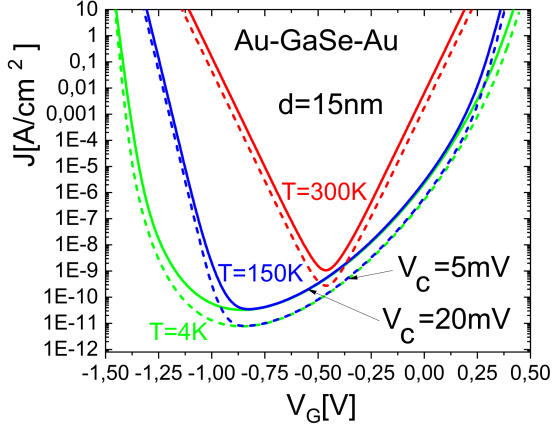


Fig. 12. Theoretical tunneling current J versus gate voltage V_G , calculated for different values of temperature for the structure Au–GaSe–Au, i.e., with medium gap channel, for applied voltage $V_C = 20$ mV (solid lines), and for $V_C = 5$ mV (dashed lines). The GaSe channel forbidden gap $E_g = 2$ eV and its width $d = 15$ nm are used. It is seen that the change in $J(V_G)$ characteristic with increasing temperature above $T = 200$ K becomes significant.

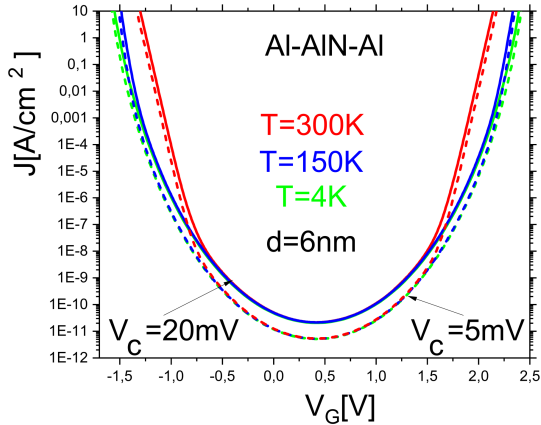


Fig. 13. Theoretical tunneling current J versus gate voltage V_G calculated for different values of temperature for the structure Al–AlN–Al, i.e., with wide gap channel, for applied voltage $V_C = 20$ mV (solid lines), and for $V_C = 5$ mV (dashed lines). The AlN channel forbidden gap $E_g = 4.2$ eV and its width $d = 6$ nm are used. It can be seen that the very strong dependence of J on V_G is preserved at least up to the temperature of $T = 300$ K.

6. Conclusions

The presented theoretical project of controlled transmission of electron current through the barrier potential can be treated as a new type of tunnel transistor without a heterojunction, unlike classic TFET. It is a simple extension of the theoretically and experimentally proven structure for studying the dependence of the tunnel current on the applied voltage (e.g., [2–7]). Its mechanism of operation

(see [10–12]) consists in controlling the height of the barrier (channel) potential polarized with a voltage V_G , i.e., controlling the current density J that tunnels through this barrier. The J change for a channel with a specific band gap value is the bigger, the bigger m_C or m_V or both, see Figs. 4 and 8. The maximum change in J , formed by tunneling electrons along the entire length of the channel, computed at helium temperature, is due to a change in V_G in the range $0 - (E_g/2e - V_C)$. For example, for $V_C = 10$ mV in the InAs structure ($d = 65$ nm), a 180 mV change in V_G means a change in J by 9 orders of magnitude. For $V_C = 10$ mV in the Au–GaSe–Au structure ($d = 15$ nm), a change in V_G by 0.6 V means a change in J by at least 12 orders of magnitude. While for $V_C = 15$ mV in the Al–AlN–Al structure ($d = 10$ nm), a change in V_G by 2 V means a change in J by at least 24 orders of magnitude. In addition, one can notice that dependence J on V_G can be adjusted by changing the voltage V_C and the width d of the channel.

Changes in the $J(V_G)$ characteristic with increasing temperature depend on the width of the band gap of the channel, and are the smaller, the wider the band gap is. A channel band gap of the order of 3 eV or more means that the relationship $J(V_G)$ in the 4–300 K range is almost unchanged, because even at the temperature $T = 300$ K, there are practically no electrons with energy about $E_F + E_G/2$, i.e., almost all electrons tunnel.

It is worth noting that the principle of operation of the described transistor model and traditional TFETs, i.e., the dependence of the energy bands of the channel on the applied voltage V_G , is the same. Similarly, the range of channel lengths used in TFETs, i.e., 15–50 nm (e.g., [17]), and in the three structures discussed above, is very similar.

The basis of this project is the invariant dependence of the electron wave vector k_z on its energy in the band gap of the channel in the considered structure. This means that a possible slight deviation of the actual shape of the barrier potential or the values of structure parameters from those adapted for calculations[†] may cause minor quantitative changes in the relation $J(V_G)$, but not qualitative ones.

References

- [1] J. Frenkel, *Phys. Rev.* **36**, 1604 (1930).
- [2] J.G. Simmons, *J. Appl. Phys.* **34**, 1793 (1963).
- [3] R. Stratton, G. Lewicki, C.A. Mead, *J. Phys. Chem. Solids.* **27**, 1599 (1966).

[†]Trapezoidal approximation of the channel potential and the $E(k)$ values of tunneling electrons calculated in the two-band model — both approximations are effective in accurately describing the measured tunneling current $J(V_G)$ in the M-I-M structures.

- [4] G.H. Parker, C.A. Mead, *Phys. Rev. Lett.* **21**, 605 (1968).
- [5] S.L. Kurtin, T.C. McGill, C.A. Mead, *Phys. Rev. B* **3**, 3368 (1971).
- [6] T.C. McGill, Ph.D. Thesis, California Institute of Technology Pasadena California, 1969.
- [7] G. Lewicki, C.A. Mead, *J. Phys. Chem. Solids.* **29**, 1255 (1968).
- [8] O. Klein, *Z. Phys.* **53**, 157 (1929).
- [9] A. Calogeracos, N. Dombey, *Contemp. Phys.* **40**, 313 (1999).
- [10] M.I. Katsnelson, K.S. Novoselov, A.K. Geim, *Nat. Phys.* **2**, 620 (2006).
- [11] Zhenglu Li, Ting Cao, Meng Wu, Steven G. Louie, *Nano Letters* **17**, 2280 (2017).
- [12] P. Pfeffer, W. Zawadzki, K. Dybko, *Semicond. Sci. Technol.* **36**, 045023 (2021).
- [13] U.E. Avci, D.H. Morris, I.A. Young, *J. Electron. Devices Soc.* **3**, 88 (2015).
- [14] D. Verreck, A.S. Verhulst, G. Groeseneken, in: *Wiley Encyclopedia of Electrical and Electronics Engineering*, 2016.
- [15] H. Ilatikhameneh, G. Klimeck, J. Appenzeller, R. Rahman, [arXiv:1603.09402v1](https://arxiv.org/abs/1603.09402v1), 2016.
- [16] C. Convertino, C.B. Zota, H. Schmid, A.M. Ionescu, K.E. Moselund, *J. Phys. Condens. Matter* **30**, 264005 (2018).
- [17] A.M. Ionescu, H. Riel, *Nature* **470**, 328 (2011).
- [18] D. Sarkar, X. Xie, W. Liu, W. Cao, J. Kang, Y. Gong, S. Kraemer, P.M. Ajayan, K. Banerjee, *Nature* **526**, 91 (2015).
- [19] W. Franz, *Ann. Phys.* **6**, 17 (1952) (in German).
- [20] Y. Taur, J. Wu, *IEEE Trans. Electron. Devices* **63**, 869 (2016).
- [21] Y.-S. Kim, K. Hummer, G. Kresse, *Phys. Rev. B* **80**, 035203 (2009).